Dissecting Apicoplast Targeting in the Malaria Parasite *Plasmodium falciparum*

Bernardo J. Foth,[1]* Stuart A. Ralph,[1]* Christopher J. Tonkin,[1]* Nicole S. Struck,[1]† Martin Fraunholz,[2] David S. Roos,[2] Alan F. Cowman,[3] Geoffrey I. McFadden[1]‡

Transit peptides mediate protein targeting into plastids and are only poorly understood. We extracted amino acid features from transit peptides that target proteins to the relict plastid (apicoplast) of malaria parasites. Based on these amino acid characteristics, we identified 466 putative apicoplast proteins in the *Plasmodium falciparum* genome. Altering the specific charge characteristics in a model transit peptide by site-directed mutagenesis severely disrupted organellar targeting in vivo. Similarly, putative Hsp70 (DnaK) binding sites present in the transit peptide proved to be important for correct targeting.

Plastid transit peptides mediate accurate targeting of many hundreds of nuclear-encoded proteins into the plastids of plants and algae (*1*, *2*), as well as into the relict plastids (apicoplasts) of malaria and related parasites (*3*–*5*). In plants, transit peptides vary in length from around 24 to over 100 amino acids, are usually enriched in serine and threonine, and exhibit an overall positive charge (*1*, *6*, *7*). Like their mitochondrial counterparts, plastid transit peptides bind Hsp70 chaperones (*8*–*10*). However, beyond these few common characteristics, plastid transit peptides are ill-defined, with no primary consensus or obvious secondary structure (*1*, *11*). In contrast to plants, protein import into the malarial plastid is a two-step process utilizing a signal peptide followed by a transit peptide (*4*, *12*). The signal peptide mediates entry into the endomembrane system, where it is cleaved off, and the transit peptide (the region immediately downstream of the signal peptide) subsequently diverts the protein away from the default secretion pathway and into the apicoplast (*12*, *13*). Several apicoplast enzymes are targets for existing antimalarial drugs, and the identification of additional apicoplast proteins should yield new drug targets (*14*).

One approach to recognizing apicoplast proteins has been through the training of the neural network PATS (*15*). Although neural networks provide reliable predictions of protein localization (*6*, *16*), they afford no insight into the underlying targeting or import mechanism and do not allow the formulation of testable hypotheses. We therefore examined a collection of putative apicoplast-targeted and non-apicoplast proteins from *Plasmodium falciparum* (*15*) to determine which characteristics of (malarial) transit peptides might be essential for plastid targeting. Transit peptides were compared to the region downstream of the predicted NH_2-terminal signal peptide (*16*) in non-apicoplast proteins (called "mature proteins") and were analyzed for amino acid composition and distribution of charge (*17*). Compared to mature proteins, malarial transit peptides are highly enriched in lysine and asparagine and depleted in acidic residues (glutamic acid and aspartic acid), especially in their first 20 amino acids (Fig. 1, fig. S1, and table S1). This results in an overall positive charge—a feature shared with plant chloroplast transit peptides (in which the positive charge is mostly due to arginine). Malarial transit peptides are also enriched in isoleucine but contain smaller amounts of small apolar amino acids [glycine, alanine, valine, and leucine (table S1)].

We then searched for features that distinguished between data sets of apicoplast-targeted and non-apicoplast proteins, with the goal of identifying apicoplast proteins from the complete *P. falciparum* genome. After prediction of the signal peptide cleavage site by the neural network tool SignalP (*16*), putative transit peptides were identified by two main features: (i) the regional net charge at their NH_2-terminus, including the nature of the first charged amino acid (basic versus acidic) [characteristics that have also been found to be important for mitochondrial transit peptides (*18*, *19*)]; and (ii) the presence of a sequence region enriched in asparagine and lysine (and its regional net charge). By assigning appropriate cutoff values, we generated several sets of rules that, in conjunction with SignalP, identified protein sequences with NH_2-terminal sequence characteristics typical of apicoplast-targeted proteins. The simplest set of rules defined a protein as "apicoplast-positive" if it met the following three criteria: (i) it started with a signal peptide, (ii) the 80 amino acids following the predicted signal peptide cleavage site con-

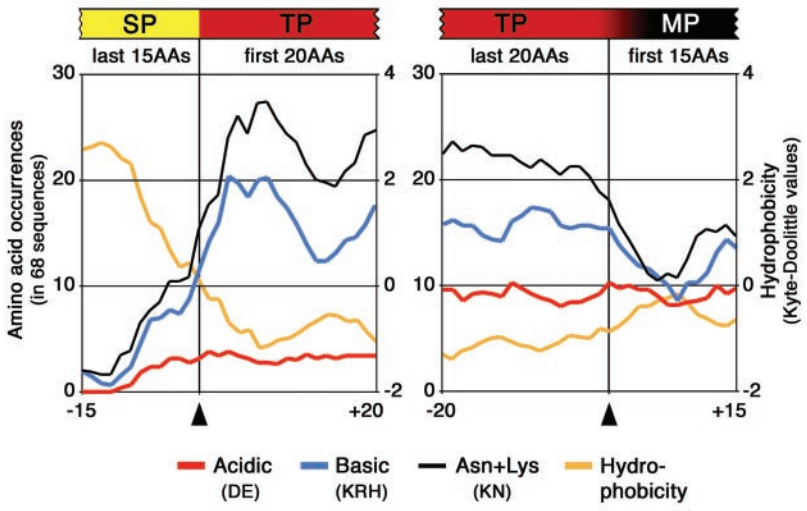

Fig. 1. Positional properties of apicoplast-targeting leaders of *P. falciparum*. Sixty-eight putative apicoplast-targeted proteins were aligned around the predicted signal peptide (SP) cleavage sites (arrowhead at bottom of left panel) and around the estimated boundaries between the transit peptide (TP) and the mature protein (MP) (*17*) (arrowhead at bottom of right panel). The graphs show average occurrences of acidic (red line) and basic (blue line) amino acids, as well as the average sum of asparagine and lysine residues (black line) (left scale on *y* axis). The yellow line indicates hydrophobicity (average Kyte-Doolittle values; right scale on *y* axis). Each value represents the mean of the 68 protein sequences at a given position, which was then averaged over five consecutive alignment positions.

[1]Plant Cell Biology Research Centre, School of Botany, University of Melbourne, Parkville, VIC 3010, Australia. [2]Department of Biology, University of Pennsylvania, Philadelphia, PA 19104, USA. [3]The Walter and Eliza Hall Institute of Medical Research, Melbourne, VIC 3050, Australia.

*These authors contributed equally to this work.
†Present address: Universität Hamburg, Zoologisches Institut und Zoologisches Museum, 20146 Hamburg, Germany.
‡To whom correspondence should be addressed. E-mail: gim@unimelb.edu.au

tained a stretch of 40 amino acids with at least nine asparagines and/or lysines, and (iii) the asparagine/lysine-enriched region had a ratio of basic residues to acidic residues of at least 5 to 3. When applied to the published training sets (*15*), this combination of rules correctly classified 72 out of 76 likely apicoplast-targeted proteins, and 97 out of 102 non-apicoplast proteins. To generate a tool that would produce a scaled rather than just a binary (yes or no) output, we combined three sets of rules based on features described above. Our tool, "PlasmoAP" (for *Plasmodium falciparum* apicoplast-targeted proteins), thus generates a score on a four-point scale denoting how well a given sequence matches the characteristics of apicoplast-targeted proteins, which in turn may indicate the likelihood of it being apicoplast-localized in vivo. This tool is described in the supporting online material and is publicly available at http://PlasmoDB.org (*20*). PlasmoAP readily discriminates apicoplast- from mitochondrion-targeted proteins, because mitochondrial proteins lack a signal peptide.

Rigorous analysis of PlasmoAP accuracy in silico is not currently possible because of the paucity of experimentally validated apicoplast proteins [only two have been verified in *P. falciparum* (*12*)]. However, an important advantage of rule-based predictors such as PlasmoAP over neural networks (*15*) is the ability to test underlying rules in vivo. We therefore carried out transit peptide mutagenesis experiments to test parameters of amino acid charge intrinsic to PlasmoAP. The wild-type bipartite leader (signal peptide plus transit peptide) of acyl carrier protein (ACP) directed green fluorescent protein (GFP) to the apicoplast in *P. falciparum* (Fig. 2A) (*12*). Consistent with the two-step mechanism of plastid targeting in apicomplexan parasites, signal peptide deletion from the ACP leader resulted in cytoplasmic GFP accumulation (Fig. 2B). Transit peptide deletion led to the secretion of GFP into the parasitophorous vacuole, which is the compartment that separates the parasite from the surrounding host erythrocyte (Fig. 2C) (*12*), providing a convenient phenotype to assay transit peptide mutants. Eliminating two positive charges from the NH_2-terminus of the ACP transit peptide (by changing two lysines into alanines at transit peptide positions 2 and 6) maintained a net positive charge in the transit peptide and did not substantially disrupt apicoplast targeting (Fig. 2D). Replacing either of these two lysine residues by glutamic acid resulted in two different phenotypes. Insertion of a negative charge at position 6 led to a small perturbation of targeting whereby most of the GFP was still trafficked to the apicoplast while a minor component accumulated in the parasitophorous vacuole (Fig. 2E), which is indicative of a slightly reduced transit peptide efficacy. In contrast, reversing the charge at the position closest to the NH_2-terminus (transit peptide position 2) drastically altered targeting, with virtually all of the GFP accumulating in the parasitophorous vacuole (Fig. 2F). Replacing both lysine residues with acidic residues completely ablated apicoplast targeting (Fig. 2, G and H) and produced a phenotype akin to that observed when the transit peptide was completely removed (Fig. 2C). The fact that glutamic acid (Fig. 2G) and aspartic acid (Fig. 2H) residues generated the same phenotype indicates that the amino acid charge was the decisive factor preventing apicoplast targeting. Signal peptides were faithfully cleaved in all mutants, and accurate processing of transit peptides (*21*) was apparent where GFP was targeted to the apicoplast (*22*).

These in vivo experiments demonstrate that both the placement of basic residues and the depletion of acidic residues in transit peptides are crucial for plastid targeting in *P. falciparum*, as has been observed in mitochondrial transit peptides (*18*, *19*). PlasmoAP was highly accurate in predicting targeting outcomes for the mutant transit peptides (Fig. 2). The mutant in which a glutamic acid replaced a lysine near the NH_2-terminus of the transit peptide (Fig. 2F) represented the

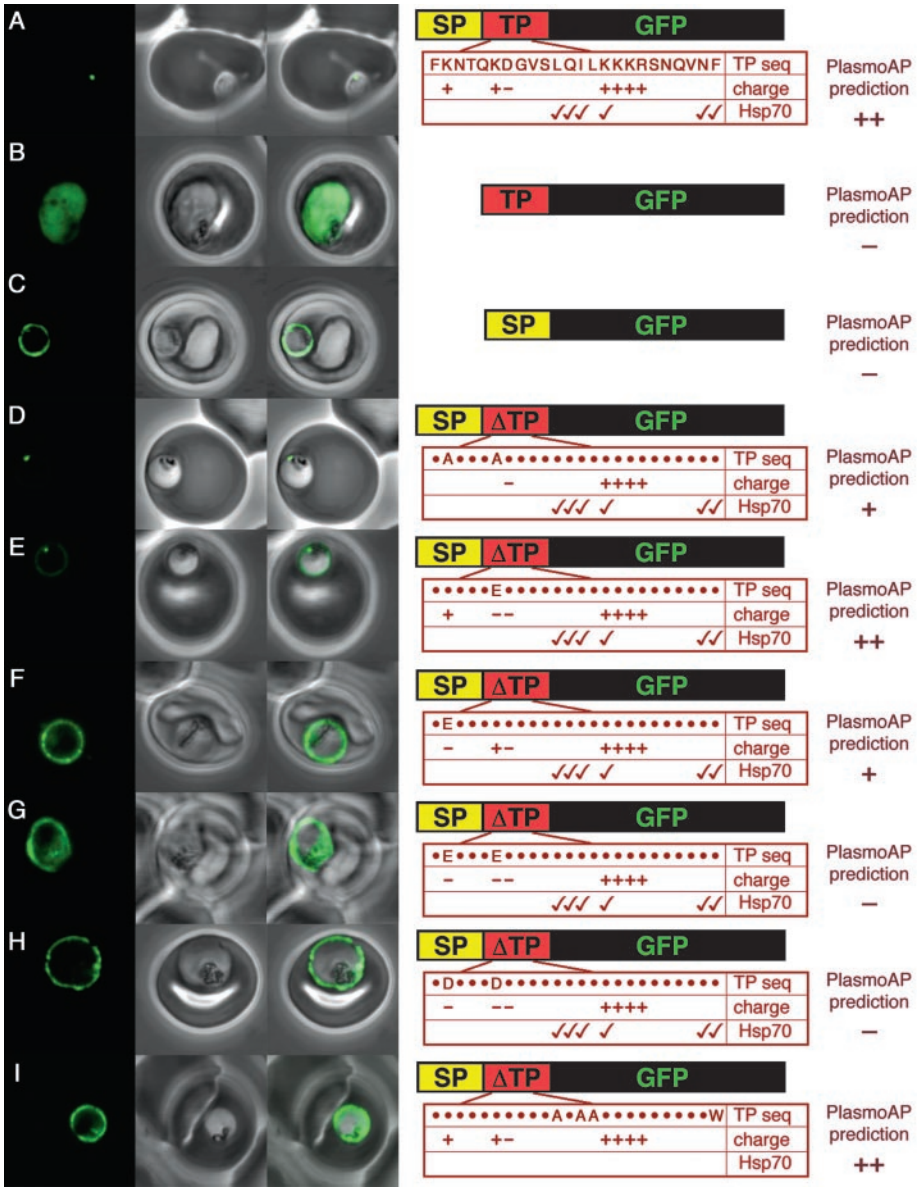

Fig. 2. GFP targeting by mutant ACP transit peptides. (**A**) Apicoplast targeting of the wild-type ACP leader. (**B**) Cytosolic targeting of a construct lacking a signal peptide. (**C**) Secretion to the parasitophorous vacuole of a construct lacking a transit peptide. The substitutions introduced into mutants (**D** to **I**) are detailed in the accompanying panels at right (*25*), where a dot (·) indicates no change. Check marks indicate putative Hsp70 binding sites. Predictions by the apicoplast protein predictor PlasmoAP are shown for each mutant. Internal labeling in (F) to (I) likely represents GFP in the food vacuole that has been taken up from the parasitophorous vacuole during phagocytosis.

only discrepancy between observed phenotypes and PlasmoAP predictions.

We then used PlasmoAP to predict how many of the 5282 proteins of the *P. falciparum* nuclear genome (*5*) are likely to be apicoplast targeted. 529 sequences received a "good" (+) or "very good" (++) PlasmoAP score (the PlasmoAP scoring system is described in the supporting online material). After manual removal of 63 proteins judged to be non-apicoplast on the basis of their previous annotation, we thus identified 466 proteins that we predict to be apicoplast-targeted. Potential apicoplast proteins thus represent a considerable subset of the 1399 proteins predicted to enter the *Plasmodium* endomembrane system (*17*). Most (77%) of the 466 PlasmoAP-predicted apicoplast proteins are also predicted to be apicoplast-targeted by the neural network PATS (*15*). Furthermore, the size and putative functions of this predicted set of proteins are congruent with current understanding of apicoplast metabolic pathways (*5*).

Another factor suggested to play a role in protein targeting to plant plastids is the binding of Hsp70 chaperones to plastid transit peptides (*8*–*10*). Putative Hsp70 binding sites can be predicted with a bioinformatic tool originally developed to predict the binding affinities of short peptides to the bacterial Hsp70 homolog DnaK (*23*), and analyses of plant transit peptides revealed an abundance of Hsp70 binding sites (*9*, *10*). Predicted Hsp70 binding sites in plant transit peptides are concentrated at two regions: approximately at amino acid 13 and amino acids 26 through 36 (*9*, *10*) (Fig. 3, inset). This same pattern is reflected in predicted apicoplast transit peptides (Fig. 3) but is absent from non-apicoplast proteins (Fig. 3). This pattern and the abundance of putative binding sites in apicoplast transit peptides (>90% of sequences) suggested that Hsp70 binding might be important to apicoplast targeting.

To test this hypothesis in vivo, we constructed another ACP transit peptide mutant, in which one isoleucine and two leucine residues were changed to alanines, and one phenylalanine was changed to tryptophan (Fig. 2I). These conservative mutations did not alter charge, hydrophobicity, or aromatic amino acid content (Fig. 2I) but drastically changed predicted Hsp70 binding affinity (fig. S3). In the Hsp70 mutant, most GFP was mistargeted to the parasitophorous vacuole, although some GFP fluorescence was still detectable in the plastid of some cells (Fig. 2I), particularly in merozoites where no parasitophorous vacuole is present (not shown in Fig. 2). Ablation of putative Hsp70 binding sites, without changing charge properties, thus led to a substantial decrease in transit peptide efficacy. The hypothesis that Hsp70 binding sites are an important component of apicoplast transit peptides might also explain a previously anomalous experimental result observed in the related apicomplexan parasite *Toxoplasma gondii*. The first 55 amino acids of the *T. gondii* ribosomal protein small subunit 9 (S9) leader target GFP to the *Toxoplasma* apicoplast, but a small COOH-terminal truncation in the transit peptide, leaving 49 amino acids, abrogates apicoplast targeting (*24*). Hence, six amino acids [RVLPLV (*25*)] of this transit peptide are vital for apicoplast targeting (*24*). These six amino acids compose an excellent hydrophobic core for a potential Hsp70 binding site (fig. S3). The *Toxoplasma* deletion construct (*24*) is thus consistent with our findings implicating Hsp70 binding to transit peptides as being important for apicoplast targeting.

Several factors limit our understanding of the importance of Hsp70 binding to transit peptide functionality. Some residual targeting to the apicoplast in the mutant transit peptide (Fig. 2I) suggests that Hsp70–transit peptide interactions are not an absolute requirement for plastid targeting and/or import but might simply increase efficacy and fidelity. As is the case in mitochondrial and plant chloroplast transit peptides (*26*), a small number (<10%) of putative apicoplast transit peptides are predicted by the existing algorithm (*23*) to lack Hsp70 binding sites, but it is unclear whether this is due to limitations in applying this tool to eukaryotic systems. It remains to be demonstrated that Hsp70 binds to apicoplast transit peptides, which has been shown for both plant chloroplast and mitochondrial transit peptides (*26*). Because of these uncertainties, Hsp70 site prediction was not incorporated into PlasmoAP. Accordingly, PlasmoAP did not correctly predict the targeting outcome for the Hsp70 mutant (Fig. 2I), which represents a current limitation as well as a future challenge for this tool.

These results suggest a simple model of plastid targeting in malaria parasites that incorporates components of mitochondrial and plant plastid protein import (*7*, *27*, *28*), as well as additional features required to explain transport across the four membranes surrounding the apicoplast (*13*). In this model, the signal peptide mediates cotranslational insertion into the endomembrane lumen and is cleaved. Endomembrane-derived vesicles dock with the outermost apicoplast membrane, delivering proteins whose NH_2-termini are maintained in an unfolded conformation by bound Hsp70 molecules (*5*). Positively charged transit peptides are electrophoretically drawn through a series of negatively charged transmembrane pores (*13*) into the reducing environment of the apicoplast lumen (*5*, *29*). Once inside, apicoplast-encoded Hsp93 (previously called Hsp100 or ClpC) (*28*, *30*) and/or Hsp70 bind to the transit peptide, preventing retrograde movement and drawing the protein into

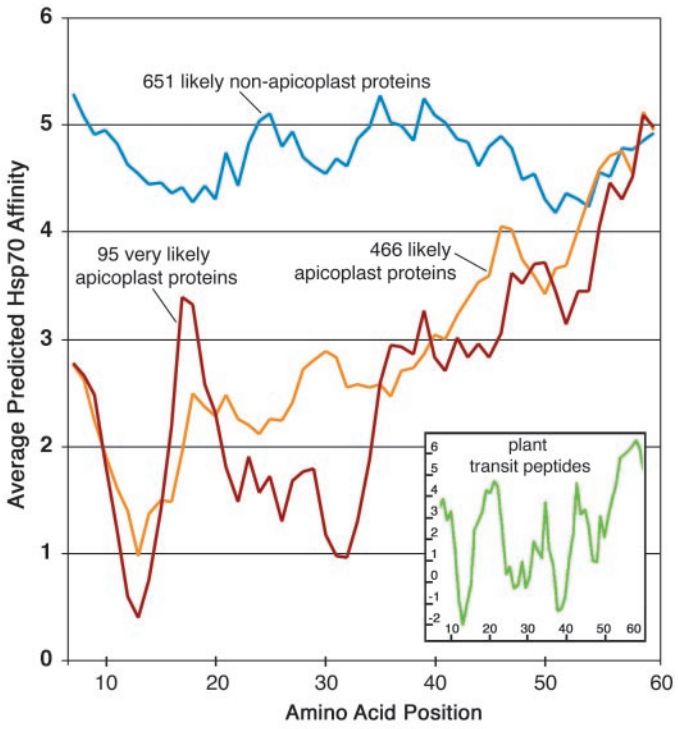

Fig. 3. Predicted Hsp70 binding affinities for putative apicoplast-targeted and non-apicoplast proteins identified in the *P. falciparum* genome. All sequences contained an NH_2-terminal signal peptide (*16*), which was removed before calculation of Hsp70 binding affinities (*23*) (expressed as free energy; lower values correspond to higher Hsp70 affinity). Thus, the binding affinities refer to the transit peptide and mature protein regions in the putative apicoplast-targeted and non-apicoplast proteins, respectively. Binding affinities were averaged for (blue line) 651 likely non-apicoplast proteins that received a negative (–) PlasmoAP score [after removal of 164 putative rifins and stevors and seven sequences that are annotated as apicoplast-targeted (*5*)], for (orange line) 466 likely apicoplast-targeted proteins that received a positive (+ and ++) PlasmoAP score (after removal of 63 sequences annotated as localized to other compartments), and for (dark red line) 95 very likely apicoplast-targeted sequences that received a positive (+ and ++) PlasmoAP score and whose annotation is suggestive of apicoplast localization. The inset (green line) shows predicted Hsp70 binding affinities for a collection of chloroplast-targeting transit peptides from plants [redrawn from (*9*)].

the apicoplast. The transit peptide is cleaved by a stromal processing peptidase (*21*), and the mature protein refolds with the assistance of the apicoplast-targeted GroEL homolog Cpn60 (*5*).

References and Notes

1. B. D. Bruce, *Biochim. Biophys. Acta* **1541**, 2 (2001).
2. The Arabidopsis Genome Initiative, *Nature* **408**, 796 (2000).
3. R. F. Waller *et al.*, *Proc. Natl. Acad. Sci. U.S.A.* **95**, 12352 (1998).
4. D. S. Roos *et al.*, *Curr. Opin. Microbiol.* **2**, 426 (1999).
5. M. J. Gardner *et al.*, *Nature* **419**, 498 (2002).
6. O. Emanuelsson, H. Nielsen, G. von Heijne, *Protein Sci.* **8**, 978 (1999).
7. P. Jarvis, J. Soll, *Biochim. Biophys. Acta* **1590**, 177 (2002).
8. R. A. Ivey 3rd, B. D. Bruce, *Cell Stress Chaperones* **5**, 62 (2000).
9. R. A. Ivey 3rd, C. Subramanian, B. D. Bruce, *Plant Physiol.* **122**, 1289 (2000).
10. D. V. Rial, A. K. Arakaki, E. A. Ceccarelli, *Eur. J. Biochem.* **267**, 6239 (2000).
11. G. von Heijne, K. Nishikawa, *FEBS Lett.* **278**, 1 (1991).
12. R. F. Waller, M. B. Reed, A. F. Cowman, G. I. McFadden, *EMBO J.* **19**, 1794 (2000).
13. G. G. van Dooren, S. D. Schwartzbach, T. Osafune, G. I. McFadden, *Biochim. Biophys. Acta* **1541**, 34 (2001).
14. S. A. Ralph, M. C. D'Ombrain, G. I. McFadden, *Drug Resist. Updates* **4**, 145 (2001).
15. J. Zuegge, S. Ralph, M. Schmuker, G. I. McFadden, G. Schneider, *Gene* **280**, 19 (2001).
16. H. Nielsen, J. Engelbrecht, S. Brunak, G. von Heijne, *Protein Eng.* **10**, 1 (1997).
17. Materials and methods are available as supporting material on *Science* Online.
18. T. S. Heard, H. Weiner, *J. Biol. Chem.* **273**, 29389 (1998).
19. L. Ni, T. S. Heard, H. Weiner, *J. Biol. Chem.* **274**, 12685 (1999).
20. J. C. Kissinger *et al.*, *Nature* **419**, 490 (2002).
21. G. G. van Dooren, V. Su, M. C. D'Ombrain, G. I. McFadden, *J. Biol. Chem.* **277**, 23612 (2002).
22. B. J. Foth *et al.*, data not shown.
23. S. Rudiger, L. Germeroth, J. Schneider-Mergener, B. Bukau, *EMBO J.* **16**, 1501 (1997).
24. S. Yung, T. R. Unnasch, N. Lang-Unnasch, *Mol. Biochem. Parasitol.* **118**, 11 (2001).
25. Single-letter abbreviations for the amino acid residues are as follows: A, Ala; C, Cys; D, Asp; E, Glu; F, Phe; G, Gly; H, His; I, Ile; K, Lys; L, Leu; M, Met; N, Asn; P, Pro; Q, Gln; R, Arg; S, Ser; T, Thr; V, Val; W, Trp; and Y, Tyr.
26. X. P. Zhang, E. Glaser, *Trends Plant Sci.* **7**, 14 (2002).
27. T. Komiya *et al.*, *EMBO J.* **17**, 3886 (1998).
28. D. Jackson-Constan, M. Akita, K. Keegstra, *Biochim. Biophys. Acta* **1541**, 102 (2001).
29. R. J. Wilson, *J. Mol. Biol.* **319**, 257 (2002).
30. _____ *et al.*, *J. Mol. Biol.* **261**, 155 (1996).

31. We thank R. Good and T. Speed for bioinformatic assistance and suggestions on PlasmoAP, M. McCarthy and R. Gleadow for assistance with statistical analysis, and G. van Dooren for critical reading of the manuscript. B.J.F. is supported by a Melbourne International Research Scholarship and a Melbourne International Fee Remission Scholarship. S.A.R. and C.J.T. are supported by Melbourne Research Scholarships. D.S.R. is a Burroughs Wellcome Scholar and an Ellison Foundation Senior Scholar in Global Infectious Diseases. G.I.M. and A.F.C. are HHMI International Scholars, and G.I.M. is an Australian Research Council Professorial Fellow. Support from U.S. NIH and the Australian Research Council and a program grant from the National Health and Medical Research Council of Australia are gratefully acknowledged.

Supporting Online Material

www.sciencemag.org/cgi/content/full/299/5607/705/DC1
Materials and Methods
SOM Text
Figs. S1 to S3
Table S1
References and Notes

19 September 2002; accepted 27 November 2002

PDGFRA Activating Mutations in Gastrointestinal Stromal Tumors

Michael C. Heinrich,[1]* Christopher L. Corless,[2] Anette Duensing,[3] Laura McGreevey,[1] Chang-Jie Chen,[3] Nora Joseph,[3] Samuel Singer,[4] Diana J. Griffith,[1] Andrea Haley,[1] Ajia Town,[1] George D. Demetri,[5] Christopher D. M. Fletcher,[3] Jonathan A. Fletcher[3,5]*

Most gastrointestinal stromal tumors (GISTs) have activating mutations in the KIT receptor tyrosine kinase, and most patients with GISTs respond well to Gleevec, which inhibits KIT kinase activity. Here we show that ~35% (14 of 40) of GISTs lacking *KIT* mutations have intragenic activation mutations in the related receptor tyrosine kinase, platelet-derived growth factor receptor α (*PDGFRA*). Tumors expressing KIT or PDGFRA oncoproteins were indistinguishable with respect to activation of downstream signaling intermediates and cytogenetic changes associated with tumor progression. Thus, *KIT* and *PDGFRA* mutations appear to be alternative and mutually exclusive oncogenic mechanisms in GISTs.

Gastrointestinal stromal tumors (GISTs) are the most common mesenchymal tumors of the gastrointestinal tract and are particularly sensitive to Gleevec, a new cancer therapy (*1–5*). Gleevec inhibits the constitutively activated form of the KIT receptor tyrosine kinase, which is the critical transforming oncoprotein in more than 85% of GISTs. Although most GISTs have activating KIT mutations, a subset are *KIT* wild type (*KIT*-WT) (*6, 7*). Notably, a high level of total KIT protein expression, which is a defining feature of GISTs (*2, 7, 8*), is not characteristic of *KIT*-WT GISTs (fig. S1). However, cells of the interstitial cells of Cajal lineage—from which GISTs are thought to arise—express KIT strongly (*2, 9*). Therefore, activation of another oncoprotein in *KIT*-WT GISTs might be accompanied by *KIT* transcriptional down-regulation.

To explore alternative receptor tyrosine kinase (RTK) oncoproteins that might participate in GIST pathogenesis, we performed immunoprecipitations with polyclonal antisera (panRTK antisera) against peptides from regions of strong sequence conservation across the family of receptor tyrosine kinases. These panRTK antisera have been extensively validated in immunoprecipitations of ERBB2, NTRK3, ALK, and KIT kinase oncoproteins from lysates of frozen human tumors (*10*). Phosphotyrosine immunostaining of panRTK immunoprecipitates from a *KIT*-WT GIST (GIST478) revealed presumptive phosphoproteins of about 150 and 170 kD, consistent with the size of immature and mature glycosylated PDGFRA, respectively (Fig. 1, A and B). We next showed that phosphorylated PDGFRA (phosphoPDGFRA) was strongly expressed and comigrated with the panRTK phosphoproteins and several of the predominant phosphorylated proteins from the GIST478 whole-cell lysate (Fig. 1, A and B). By contrast, KIT was not demonstrably phosphorylated. Therefore, phosphoPDGFRA appeared to be the predominant phosphoRTK in GIST478.

Mutually exclusive phosphoKIT and phosphoPDGFRA expression was demonstrated, respectively, in a GIST with a KIT juxtamembrane region mutation and another *KIT*-WT GIST (Fig. 1, C to E). We then confirmed differential phosphoPDGFRA expression in three *KIT*-WT and two *KIT*-mutant GISTs. PhosphoPDGFRA expression was restricted to the *KIT*-WT GISTs, where KIT expression was low to undetectable (Fig. 1, F to H). Likewise, PDGFRA expression was low to undetectable in ~70% of *KIT*-mutant GISTs (fig. S2). Confirmation of GIST diagnosis in *KIT*-WT GISTs was enabled by immunostaining for protein kinase C θ (fig. S3).

We identified *PDGFRA* activation loop (exon 18) mutations in the three *KIT*-WT GISTs that expressed phosphoPDGFRA (Fig. 1). Two of the *KIT*-WT GISTs had an identical *PDGFRA* missense mutation, leading to substitution of valine for the highly conserved aspartic acid at codon 842 (PDGFRA D842V) (*11*). The other *KIT*-WT GIST had an in-frame deletion, resulting in loss of PDGFRA amino acid residues 842 to 845 (DIMH). These *PDGFRA* mutations (Table 1) (figs. S4 to S6) are homologous to those responsible for KIT and FMS-

[1]Department of Medicine, [2]Department of Pathology, Oregon Health & Science University Cancer Institute and Portland VA Medical Center, Portland, OR 97201, USA. [3]Department of Pathology, Brigham and Women's Hospital, 75 Francis Street, Boston, MA 02115, USA, and Harvard Medical School, Boston, MA 02115, USA. [4]Department of Surgery, Memorial Sloan-Kettering Cancer Institute, New York, NY 10021, USA. [5]Department of Medical Oncology, Dana-Farber Cancer Institute and Harvard Medical School, Boston, MA 02115, USA.

*To whom correspondence should be addressed. E-mail: heinrich@ohsu.edu, jfletcher@partners.org